Theoretical study on adsorption and reaction of polymeric formic acid on the Cu(111) surface

Septia Eka Marsha Putra,[1,2] Fahdzi Muttaqien,[3,4] Yuji Hamamoto,[1,5] Kouji Inagaki,[1,5] Akitoshi Shiotari,[6,*] Jun Yoshinobu,[7] Yoshitada Morikawa,[1,5,8] and Ikutaro Hamada[1,5,†]

[1]*Department of Precision Engineering, Graduate School of Engineering, Osaka University, 2-1 Yamada-oka, Suita, Osaka 565-0871, Japan*
[2]*Department of Engineering Physics, Institut Teknologi Sumatera, Jalan Terusan Ryacudu, Way Hui, Jati Agung, South Lampung, 35365, Indonesia*
[3]*Instrumentation and Computational Physics Research Group, Faculty of Mathematics and Natural Sciences, Institut Teknologi Bandung, Jalan Ganesha 10, Bandung, West Java 40132, Indonesia*
[4]*Master Program in Computational Science, Faculty of Mathematics and Natural Sciences, Institut Teknologi Bandung, Jalan Ganesha 10, Bandung, West Java 40132, Indonesia*
[5]*Elements Strategy Initiative for Catalysts and Batteries (ESICB), Kyoto University, Goryo-Ohara, Nishikyou-ku, Katsura, Kyoto 615-8245, Japan*
[6]*Department of Advanced Materials Science, The University of Tokyo, 5-1-5 Kashiwanoha, Kashiwa, Chiba 277-8561, Japan*
[7]*The Institute for Solid State Physics, The University of Tokyo, 5-1-5 Kashiwanoha, Kashiwa, Chiba 277-8581, Japan*
[8]*Research Center for Precision Engineering, Graduate School of Engineering, Osaka University, 2-1 Yamada-oka, Suita, Osaka 565-0871, Japan*

(Received 6 April 2021; revised 20 May 2021; accepted 15 June 2021; published 6 July 2021)

We investigate the polymeric adsorption of formic acid (HCOOH) on the Cu(111) surface by means of density functional theory. We present structural models for the polymeric form of HCOOH on Cu(111) and characterize their stability, electronic, and vibrational properties. Based on the energetics and dynamics, as well as simulated scanning tunneling microscopy and atomic force microscopy images, we propose that the α polymorph is likely to be formed on the Cu(111) surface and can explain the experimental findings. We also study the initial step of the catalytic dehydrogenation of HCOOH and find that the O-H bond dissociation at the edge of the polymer is facilitated, rather than that forming hydrogen bonding, agreeing well with the experiments.

DOI: 10.1103/PhysRevMaterials.5.075801

I. INTRODUCTION

Hydrogen is one of the promising renewable energy sources to replace the fossil fuels and to reduce carbon emission, and to realize a sustainable society. Proton exchange membrane fuel cells (PEMFCs) are used to generate electricity by reacting hydrogen with oxygen to emit water only. Conventional PEMFCs use the compressed hydrogen gas as fuel, and there are safety concerns (such as flammability) during storage and transportation. As an alternative, other materials have been investigated to store hydrogen for use in the fuel cells. One of the promising candidates is formic acid (HCOOH) [1–3]. Formic acid exists as a stable molecule at standard temperature and pressure conditions, is nontoxic, and shows a low crossover rate through the Nafion membrane, making it a promising material to solve the safety issues in the fuel cell technology. In general, HCOOH can be catalytically converted into CO_2 and H_2 via dehydrogenation or into CO and H_2O via dehydration. On the low index metal surfaces (i.e., Pd [4,5], Pt [6–8], Ag [9], and Cu [10–13]), HCOOH is known to be selectively decomposed into CO_2 and H_2 via the formate species (HCOO), which is an important reaction intermediate for the methanol synthesis and hydrogen generation. Therefore, adsorption and catalytic reactions of HCOOH on those surfaces have been investigated extensively.

The HCOOH is found to form polymeric structures when exposed to clean surfaces at low temperature [9–12,14]. Columbia *et al.* [14] studied HCOOH adsorption on Pt(111) by using high energy electron loss spectroscopy and infrared reflection absorption spectroscopy (IRAS) and proposed the formation of overlayer in α and β polymorphs, depending on the coverage and temperature (see Fig. 1 for the schematic structures). On clean Ag(111), by using a combination of reflection absorption infrared spectroscopy (RAIRS) and temperature programmed desorption (TPD), similar polymeric HCOOH was also reported [9]. Baber *et al.* [10] investigated HCOOH on Cu(111) by using IRAS, scanning tunneling microscopy (STM), x-ray photoelectron spectroscopy (XPS), and near edge x-ray absorption fine structure spectroscopy, and found that HCOOH is assembled to form a polymeric chain. Based on the characteristic vibrational modes (out-of-plane O−H deformation and C=O stretching) they concluded that α-polymeric HCOOH chains are formed, which is then deprotonated to form HCOO by annealing. Shiozawa *et al.* [12] studied desorption and deprotonation kinetics of HCOOH on Cu(111) by using TPD, XPS, and time-resolved

*Present address: Department of Physical Chemistry, Fritz-Haber Institute of the Max-Planck Society, Faradayweg 4-6, D-14195, Berlin, Germany.
†ihamada@prec.eng.osaka-u.ac.jp

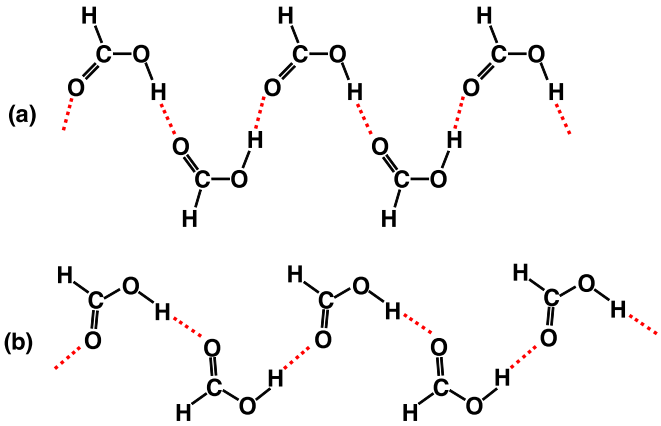

FIG. 1. Schematic structures of (a) α-polymeric and (b) β-polymeric HCOOH. The red dashed line between the HCOOH molecules represents the hydrogen bonding in the polymeric structures.

IRAS, and they also assigned the structure of adsorbed HCOOH to the α-polymeric form. On the other hand, Marcinkowski *et al.* [11] conducted temperature programmed desorption/reaction (TPD/R) and high-resolution STM experiments and concluded that the β-polymeric HCOOH is formed on Cu(111) based on the distance between the bright spots in the acquired STM images. Apparently, there is a contradicting conclusion in the literature, in terms of the polymeric structure of HCOOH on Cu(111), which calls for further experimental and theoretical research. The proposed structural models of the α and β polymers are based on crystalline HCOOH and composed of trans-HCOOH, and the difference between these polymer lies in the relative position and orientation. The β polymer was derived from crystalline HCOOH in the β form, initially proposed by Holtzberg *et al.* [15], and later reinvestigated by Nahringbauer *et al.* [16] On the other hand, the α form was postulated by the Mikawa *et al.* [17,18] to explain the doublet peak observed in IRAS, but the actual structure has not been reported. Aside from the controversies over the stable polymorphs of crystalline HCOOH, we here focus on the overlayer structures in the α and β forms on the surface. Despite a large number of studies on HCOOH adsorbed on various metal surfaces, we consider the HCOOH on Cu, since it is inexpensive, low CO poisoning, and various analyses for polymeric HCOOH have been conducted that can be used as references.

On the theoretical side, a number of studies have also been conducted to investigate the adsorption and decomposition of HCOOH on the Cu(111) surface [5,8,13,19–24]. Most of the studies considered monomeric HCOOH (i.e., single molecule), and there have been no theoretical investigation of polymeric HCOOH on Cu(111). Recently, Chen *et al.* [25,26] investigated the decomposition of hydrogen-bonded HCOOH's on a number of surfaces and demonstrate the importance of hydrogen bonding in the catalytic reaction of HCOOH. Furthermore, the edges of the polymeric structures have been reported to play a key role in the dehydrogenation process [10]. Yet, the detailed structure and the catalytic reaction of the polymeric HCOOH are to be clarified. Very recently, we investigated the structures of polymeric HCOOH as well as assemblies of HCOOH/HCOO and HCOO on Cu(111) by combining high-resolution STM, noncontact atomic force microscopy (AFM), and density functional theory (DFT) [27].

In this work, we expand on the polymeric HCOOH and describe the models for the α- and β-polymeric forms of HCOOH on Cu(111) in detail, and discuss their stability, electronic and vibrational properties, and dehydrogenation by means of DFT. We consider polymeric HCOOH in the forms of the infinite chain (overlayer) and finite cluster on the surface to study the bulk and edge of the polymeric structures. We also simulate the IRAS spectra as well as STM and AFM images based on the structures discussed here. The natures of the HCOOH polymorphs on Cu(111) are discussed in detail.

II. METHODS

Electronic structure calculations were performed by using the STATE code [28], which has been used to investigate adsorption and catalytic reactions such as HCOOH adsorption and decomposition [24], HCOO adsorption and hydrogenation [29,30], and formate decomposition [31]. The electron-ion interactions were described by using the ultrasoft pseudopotentials [32]. Wave functions and charge density were expanded in terms of a plane wave basis set with the kinetic energy cutoffs of 36 Ry and 400 Ry, respectively. For the exchange-correlation functional, we used the rev-vdW-DF2 [33,34] as implemented [35] in the STATE code. This functional has been shown to predict accurate adsorption energy of HCOOH on Cu(111) [24]. The Cu(111) surface was modeled by using a three-monolayer-thick slab. Adsorbate and the top two layers were allowed to relax until the forces acting on atoms became smaller than 5.14×10^{-2} eV/Å (1×10^{-3} Hartree/Bohr), while the atoms in the bottom-most layer were fixed to their respective bulk positions. We performed the calculations by using thicker four- and six-layer slabs, and confirmed that the change in the adsorption energy is less than 10 meV. To minimize the artificial electrostatic interaction between the image slabs, a 31-Å-thick vacuum was introduced. We also performed calculations by using the effective screening medium (ESM) method [36,37], which eliminates the artificial electrostatic interaction between the image slabs, and confirmed that the error in the adsorption energy associated with the use of the periodic boundary condition is less than 10 meV. We modeled infinite polymeric structure as well as finite polymeric clusters of HCOOH in the α and β forms. For the infinite polymeric HCOOH structures, we employed a $(\sqrt{21} \times \sqrt{7})$ supercell, while for the finite clusters, a (5×5) one was used. For comparison, we performed calculations of monomeric HCOOH in a (5×5) supercell. The surface Brillouin zone was sampled by using 3×5 and 2×2 k-point grids for the former and the latter supercells, respectively. The harmonic vibrational frequencies were obtained by diagonalizing the mass weighted Hessian matrix, which was calculated by using the finite difference method. Only the vibrational frequencies at the Γ point were considered, because of the relatively large supercell used in our simulation. We then calculated the IRAS spectra of HCOOH's on the Cu(111) surface. The intensities were calculated from the squared dynamic dipole moments, which were estimated by the work

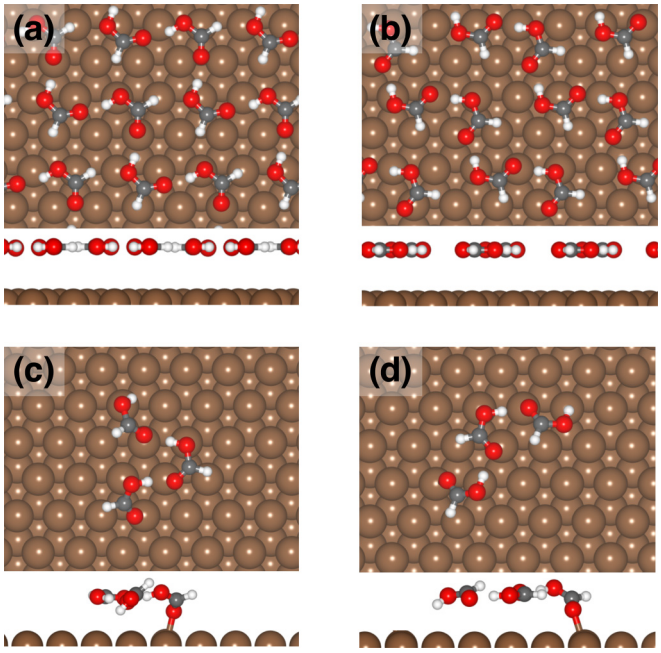

FIG. 2. Adsorption configurations of (a) infinite α-polymeric, (b) infinite β-polymeric, (c) finite α-polymeric, and (d) finite β-polymeric HCOOH's on the Cu(111) surface. The upper (lower) panel shows a top (side) view. The brown, gray, red, and white spheres represent the copper, carbon, oxygen, and hydrogen atoms, respectively.

function changes induced by the atomic displacements for each mode [38]. The ESM method [36,37] was used to calculate the work function change. The activation energy for the dehydrogenation of HCOOH was calculated by using the climbing-image nudged elastic band method [39,40].

III. RESULTS

A. Adsorption state of polymeric HCOOH on Cu(111)

In this study, we modeled the α- and β-polymeric HCOOH's on Cu(111) based on the experimental high resolution STM and AFM images [10,11,27]. Although the polymeric HCOOH was found to be incommensurate with respect to the underlying Cu(111) substrate, the polymeric structures were modeled/approximated by employing periodically repeated HCOOH structures containing four HCOOH molecules in a Cu(111) ($\sqrt{21} \times \sqrt{7}$) supercell. We examined a number of structures and determined the most stable adsorption structures of α- and β-polymeric HCOOH on Cu(111) as shown in Figs. 2(a) and 2(b), respectively. We found that polymer in ($\sqrt{21} \times \sqrt{7}$) supercell gives the lowest energy among the supercells considered in this work (see S6 in Supplemental Material [41]). In both α- and β-polymeric HCOOH structures, HCOOH molecules adsorb with their molecular plane parallel to the surface and with their carbon (C) atoms located near the fcc or hcp hollow site, and both oxygen (O) atoms, on or close to the atop sites of surface Cu atoms. The average surface-molecule distances are 3.48 Å and 3.49 Å for α- and β-polymeric HCOOH structures, respectively, implying that the interaction between the surface and the molecular layer is considerably weak. We confirmed that the optimized geometries are the equilibrium ones by calculating the total energies as functions of molecule-surface (molecular layer) distance (Supplemental Material, Fig. S1 [41]). We also performed the calculations of the finite HCOOH clusters in the α and β forms containing three HCOOH molecules in a (5 × 5) supercell, which are extracted from the infinite polymeric structures [Figs. 2(c) and 2(d), respectively]. After the structural optimization, the HCOOH molecules in the edges of the finite α-polymeric HCOOH cluster were found to be tilted, while other molecules remain flat. On the other hand, finite β-polymeric HCOOH remains almost flat after the structural optimization, but the edges of HCOOHs are slightly tilted.

TABLE I. Calculated adsorption energies per HCOOH of monomeric and polymeric HCOOH on the Cu(111) surface ($E_{\rm ads}$). The zero-point energy (ZPE) was taken into account, and those without the ZPE correction are given in parentheses. The calculated surface-molecule ($E_{\rm ads}^{\rm surf-mol}$) and molecule-molecule ($E_{\rm ads}^{\rm mol-mol}$) adsorption energies are also shown. For $E_{\rm ads}^{\rm surf-mol}$ and $E_{\rm ads}^{\rm mol-mol}$, the ZPE correction is not taken into account. In the case of monomeric HCOOH, parallel (Para) and perpendicular (OH-Perp) configurations are considered. The unit of energy is eV/HCOOH.

	Monomer		Infinite polymer		Finite polymer	
	Para	OH-Perp	α	β	α	β
$E_{\rm ads}$	−0.19	−0.44	−0.55	−0.68	−0.44	−0.49
	(−0.20)	(−0.44)	(−0.59)	(−0.71)	(−0.46)	(−0.52)
$E_{\rm ads}^{\rm surf-mol}$	−0.20	−0.44	−0.17	−0.16	−0.28	−0.24
$E_{\rm ads}^{\rm mol-mol}$	–	–	−0.42	−0.55	−0.18	−0.28

We then calculated the adsorption energy of polymeric HCOOH defined by

$$E_{\rm ads} = \frac{1}{n}\{E_{\rm tot}[({\rm HCOOH})_n/{\rm Cu}(111)] - E_{\rm tot}[{\rm Cu}(111)] - nE_{\rm tot}({\rm HCOOH})\}, \quad (1)$$

where n is the number of HCOOH molecules in the supercell, $E_{\rm tot}[({\rm HCOOH})_n/{\rm Cu}(111)]$, $E_{\rm tot}[{\rm Cu}(111)]$, and $E_{\rm tot}({\rm HCOOH})$ are total energies of the adsorbed system, the clean surface, and the HCOOH molecule in the gas phase, respectively. The calculated $E_{\rm ads}$'s for polymeric HCOOH on Cu(111) are summarized in Table I, along with those for monomeric HCOOH's. We found that $E_{\rm ads}$ for the infinite β-polymeric HCOOH is slightly larger than that of the α one, meaning that β-polymeric HCOOH is more stable on Cu(111). The calculated $E_{\rm ads}$'s after ZPE correction for the α- and β-polymeric HCOOH are −0.55 eV and −0.68 eV, respectively, which are 0.11–0.24 eV larger than that of the monomeric ones, implying that the stabilization of the polymeric structures is due to the attractive interaction with neighboring molecules. We note that the value of $E_{\rm ads}$ in the present work is different from that reported in Ref. [27], although the structure of the α polymorph is exactly the same. This is because (i) ZPE was not taken into account in Ref. [27], and (ii) in order to compare the $E_{\rm ads}$'s of different phases (mixtures of HCOOH and HCOO with various coverages and compositions), it was corrected by using the monomer HCOOH adsorption in a

much larger unit cell (see Supplemental Material [41] for further detail). The $E_{\rm ads}$'s for the finite polymeric HCOOHs show a similar trend to the infinite ones. The finite β-polymeric HCOOH is slightly more stable than the α-polymeric one, but the energy difference is much smaller than the finite ones. This suggests the competing nature of the HCOOH polymorphs on the Cu(111) surface. We also calculated $E_{\rm ads}$'s by using different exchange-correlation functionals and confirmed that our conclusions are unchanged (see Supplemental Material [41]). Furthermore, we performed calculations of free-standing polymeric HCOOH structures with rev-vdW-DF2 and found that the β-polymeric structure is more stable [41], in line with the accurate quantum chemistry calculation results for the one-dimensional HCOOH chains by Hirata [42].

The $E_{\rm ads}$ discussed above includes contributions of both surface-molecule and molecule-molecule interactions. To quantify their contributions and gain insight into the mechanism of the stability of the polymeric HCOOH, we decompose $E_{\rm ads}$ into the surface-molecule ($E_{\rm ads}^{\rm surf-mol}$) and molecule-molecule ($E_{\rm ads}^{\rm mol-mol}$) adsorption energies defined by

$$E_{\rm ads}^{\rm surf-mol} = \frac{1}{n}(E_{\rm tot}[({\rm HCOOH})_n/{\rm Cu}(111)] - E_{\rm tot}[{\rm Cu}(111)] - E_{\rm tot}[({\rm HCOOH})_n]), \quad (2)$$

and

$$E_{\rm ads}^{\rm mol-mol} = \frac{1}{n}\{E_{\rm tot}[({\rm HCOOH})_n] - nE_{\rm tot}({\rm HCOOH})\}, \quad (3)$$

where $E_{\rm tot}[({\rm HCOOH})_n]$ is the total energy of the HCOOH layer calculated in its adsorption configuration. The calculated adsorption energies are summarized in Table I. In both infinite α- and β-polymeric phases, $E_{\rm ads}^{\rm surf-mol}$'s are slightly smaller than $E_{\rm ads}$ of the flat-lying (parallel) monomeric HCOOH, and $E_{\rm ads}^{\rm mol-mol}$'s are much larger than $E_{\rm ads}^{\rm surf-mol}$'s, suggesting that the surface-molecule interaction is very weak and polymer formation is favorable, and that $E_{\rm ads}^{\rm mol-mol}$ is a dominant factor determining the stability of the polymeric structure. For the finite polymeric structures, $E_{\rm ads}^{\rm surf-mol}$'s are larger than $E_{\rm ads}$ of the flat-lying monomeric HCOOH. This is because one of the O atoms in an edge HCOOH interacts more strongly with the surface than the flat-lying monomer of polymeric structures, which can be inferred from the facts that the structure is slightly distorted (Fig. 2), and that the more distorted finite α structure has larger $E_{\rm ads}^{\rm surf-mol}$. The molecular distortion caused by the stronger surface-molecule interaction induces the weakening of the intermolecular interaction, resulting in the smaller $E_{\rm ads}^{\rm mol-mol}$'s.

To further investigate the intermolecular interaction, i.e., hydrogen bonding between HCOOH molecules, we calculated the charge density difference for the polymeric structures defined by

$$\Delta\rho(\mathbf{r}) = \rho_{({\rm HCOOH})_n/{\rm Cu}(111)}(\mathbf{r}) - \rho_{{\rm Cu}(111)}(\mathbf{r}) - \sum_i^n \rho_{\rm HCOOH}^i(\mathbf{r}), \quad (4)$$

where $\rho_{({\rm HCOOH})_n/{\rm Cu}(111)}(\mathbf{r})$, $\rho_{{\rm Cu}(111)}(\mathbf{r})$, and $\rho_{\rm HCOOH}^i(\mathbf{r})$ are the electron densities of the combined system, substrate, and ith HCOOH molecule, respectively. All the electron densities

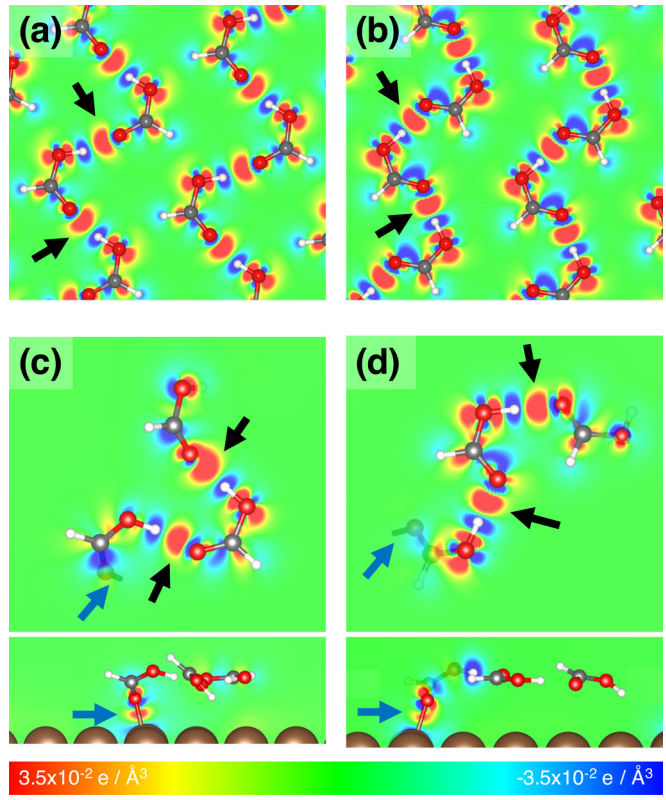

FIG. 3. Charge density differences ($\Delta\rho$) for (a) infinite α-polymer, (b) infinite β-polymer, (c) finite α-polymer, and (d) finite β-polymer HCOOH on Cu(111). $\Delta\rho$'s in the plane containing molecular planes (top view) or carboxyl group (side view) are plotted. The upper (lower) panels in (c) and (d) show the top (side) views. Maximum and minimum values are 3.5×10^{-2} $e/$Å^3 and -3.5×10^{-2} $e/$Å^3, respectively. The dark arrows indicate the polarization between the HCOOH molecules in the polymer, and dark blue arrows indicate the polarization between HCOOH and underlying substrate.

were calculated for their respective adsorption configurations. A previous study [43] reported that the intermolecular interaction of HCOOH is determined by strong hydrogen bonds, originating from the significant attractive interaction between the hydrogen atom attached to an electronegative atom (O atom), and another electronegative atom. As can be seen in Fig. 3, all the polymeric HCOOH structures exhibit charge polarization between OH and carboxyl groups (OH$\cdots$OC), implying the formation of hydrogen bondings between HCOOH molecules. In the infinite polymer structures [Figs. 3(a) and 3(b)], there is no considerable charge polarization between surface and molecules, which indicates their weak interaction, and is consistent with the calculated adsorption energy. On the other hand, the finite polymeric clusters [Figs. 3(c) and 3(d)], in particular, the finite α-polymeric HCOOH shows the sizable charge polarization between the O atom and Cu atom underneath. This indicates stronger HCOOH-substrate interaction in the finite α-polymeric HCOOH and agrees well with the calculated $E_{\rm ads}^{\rm surf-mol}$. In the finite polymeric clusters, there are dangling hydroxyl and carboxyl groups, leading to smaller $E_{\rm ads}^{\rm mol-mol}$'s and thus the smaller $E_{\rm ads}^{\rm mol-mol}$'s than those of the infinite ones.

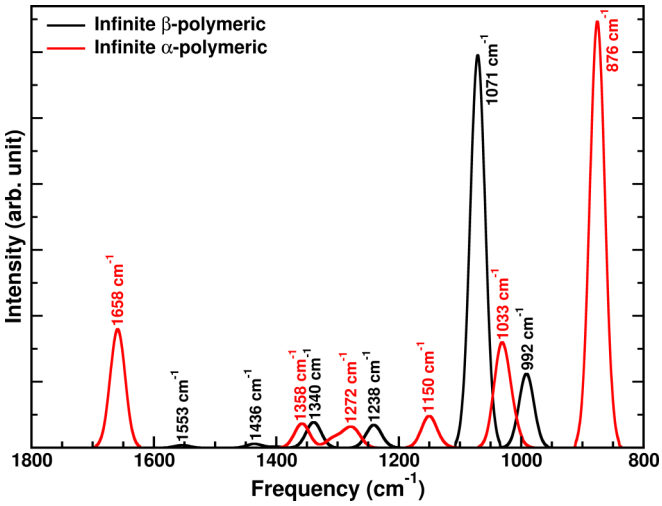

FIG. 4. Calculated IRAS of the infinite α-polymeric (red solid line) and β-polymeric (black solid line) HCOOH on Cu(111).

1. Vibrational modes and IRAS spectra

In the previous studies, the structure of the polymeric HCOOH was determined based on the measured IRAS spectra: Baber *et al.* [10] observed a distinct vibrational feature at 975 cm^{-1}, which was assigned to the out-of-plane OH deformation [π(O−H)], based on the assignment of the π(O−H) mode of the polymeric formic acid on Pt(111) by Columbia *et al.* [14], they concluded that α-polymeric HCOOH is formed on Cu(111). They also observed characteristic out-of-plane CH deformation [π(C−H)] at 1084 cm^{-1}, C=O stretching [ν(C=O)] at 1720 cm^{-1}. Shiozawa *et al.* [12] observed similar vibrational frequencies for π(O−H), π(C−H), ν(C=O) at 980 cm^{-1}, 1080 cm^{-1}, and 1709 cm^{-1}, respectively, which supports the formation of the α-polymeric HCOOH on Cu(111). Note, however, that Marcinkowski *et al.* [11] proposed the formation of the β-polymeric HCOOH based on the high resolution STM experiment.

We performed the vibrational mode analyses and IRAS simulations for both α- and β-polymeric structures on Cu(111). The simulated IRAS of the infinite polymeric HCOOH structures on the surface are shown in Fig. 4, and the assignment of the characteristic vibrational modes are summarized in Table II. Each vibrational mode are visualized and can be found in Ref. [41]. We also calculated the vibrational frequencies and IRAS for the finite polymeric HCOOH structures for comparison (see Supplemental Material [41]). For the infinite α-polymeric HCOOH, we obtained the vibrational frequencies in the range of 862–876 cm^{-1} and 1014–1033 cm^{-1}, which are assigned to π(O−H) and π(C−H), respectively, and ν(C=O)'s appear in the range of 1658–1717 cm^{-1} (Table II). Characteristic π(O−H), π(C−H), ν(C=O) peaks can be found at 877 cm^{-1}, 1033 cm^{-1}, and 1658 cm^{-1} in the simulated IRAS (Fig. 4). On the other hand, peaks for π(O−H), π(C−H), and ν(C=O) of the infinite β polymeric are found in the range of 1058–1085 cm^{-1}, 975–992 cm^{-1}, and 1553–1683 cm^{-1}, respectively. Overall, the calculated vibrational frequencies of π(O−H) and π(C−H) for α-polymeric HCOOH are lower than for the β one, whereas those for ν(C=O) are higher for the former than the latter. The calculated vibrational frequencies for the α-polymeric HCOOH are smaller than the experimental ones, but the peak assignments, relative vibrational frequencies, and relative IRAS intensities of π(O−H), π(C−H), and ν(C=O) are consistent with the experimental results by Shiozawa *et al.* [12]. On the other hand, the absolute vibrational frequencies for the β polymeric one seem to be in better agreement with the experimental values, but the order of π(O−H) and π(C−H) frequencies are reversed (relative intensities agree with the experiment) and the intensities of ν(C=O) modes are negligibly small.

Our results indicate that the α structures reproduce the vibrational signatures well: Although the absolute vibrational frequencies are underestimated, relative frequencies and relative IR peak heights agree well with the experimental findings. The possible reasons for the error in the vibrational

TABLE II. Calculated vibrational frequencies of infinite polymeric HCOOH structures adsorbed on Cu(111), along with the experimental values. The values in boldface refer to those with high IRAS intensities. See Fig. 4.

	Mode	Frequencies (cm^{-1})
α	π(O−H)	862, 872, **876**, 877
	π(C−H)	1015, 1018, 1026, **1033**
	δ(O−H)	1130, 1136, **1150**, 1160, 1263, **1272**, 1286, 1308
	δ(C−H)	1354, 1355, **1358**, 1376
	ν(C=O)	**1658**, 1663, 1702, 1716
β	π(O−H)	1058, **1071**, 1081, 1086
	π(C−H)	976, 978, 989, **992**
	δ(O−H)	1396, 1405, 1427, **1436**
	δ(C−H)	1213, 1216, **1238**, 1245, 1332, 1337, 1338, **1340**
	ν(C=O)	**1553**, 1562, 1662, 1684
Expt.	π(O−H)	975 [a], 980 [b]
	π(C−H)	1084 [a], 1080 [b]
	ν(C=O)	1720 [a], 1709 [b]

[a]IRAS spectra taken from Ref. [10].
[b]IRAS spectra taken from Ref. [12].

frequencies are as follows: The infinite polymeric structure models presented in this work are commensurate with the underlying substrate, whereas the polymeric HCOOH observed in the experiments is incommensurate. Use of a commensurate model may lead to tensile/compressive strain to the HCOOH overlayer, which affects the strength of the intermolecular hydrogen bonding and hence the vibrational frequency of the π(O−H) mode, leading to the discrepancy with the experiment. In our simulation, estimated intra- and inter-molecular-chain distances are 6.77 Å and 5.91 Å, respectively, whereas those estimated in the experiment are 6.51 Å, and 5.51 Å, respectively, and the calculated intermolecular distances are slightly larger. We calculated the vibrational frequencies of the free-standing two-dimensional HCOOH layers in the α and β forms, and found that the vibrational frequencies for the out-of-plane π(O−H) and π(C−H) increase slightly when the intra-molecular-chain distance is decreased, while the change in the inter-molecular-chain distance does not affect the vibrational frequencies significantly, because of the weak interchain interaction, of the order of few tens of meV. Unfortunately, the changes in the vibrational frequencies are not large enough to reach the agreement with the experimental values. We can see that the vibrational frequency of the π(O−H) mode in the α form is particularly underestimated. It was reported that vdW-DF tends to overestimate the hydrogen bonding strength of extended systems (2D/3D ice) [44], and for the α-polymeric HCOOH, hydrogen-bonding strength may also be overestimated, which results in the O-H bond elongation and lowering of the vibrational frequencies. In addition, we found that the frequency of the π(O−H) mode is very sensitive to the direction of hydrogen bonding and moreover, to the balance between surface-molecule ($E_{\rm ads}^{\rm surf-mol}$) and molecule-molecule ($E_{\rm ads}^{\rm mol-mol}$) interactions. Thus, we may need more accurate electronic structure and/or vibrational theory to obtain better agreement with the experiment.

2. *Simulated STM and AFM images*

We also simulated the STM images by using the Tersoff-Hamann theory [45–48] as well as AFM images by using the probe-particle method [49,50], based on our optimized infinite polymeric HCOOHs on Cu(111) (Fig. 5). The simulated STM images for α and β polymers look very similar, but by a closer look at the protrusion shapes, the simulated STM image for the α polymer is found to be in better agreement with those by Marcinkowski *et al.* [11] and by Shiotari *et al.* [27], in particular, the round edge parts of the zig-zag chains. In the AFM simulation, the HCOOH molecules are imaged as connected boomerang-shaped protrusions, and the buckling angle between the neighboring molecules is much larger in the β polymer than α polymer, and the AFM image for the α polymer is in good agreement with the experimental image by Shiotari *et al.* [27]. These results lead us to conclude that the structure of the adsorbed HCOOH on Cu(111) can be well explained by the α-polymeric form.

B. Dehydrogenation of polymeric HCOOH

Finally, we investigated the dehydrogenation of HCOOH in the polymeric HCOOH structures on Cu(111). We assumed that one of the HCOOH molecules in the α- or β-polymeric structures decomposes into bidentate HCOO (bi-HCOO) configuration, in which the HCOO molecule adsorbs in the perpendicular configuration with two O atoms adsorbed on top of Cu atoms. The decomposition process is essentially the same as that for the flat-lying monomeric HCOOH discussed in Ref. [24]. We took the most stable polymeric HCOOH structure as the initial state (IS), and for the final state (FS), we choose the bi-HCOO with the H atom in the fcc-hollow site. At the transition state (TS), the HCOOH molecule is in the perpendicular configuration with the OH bond elongated. The structures of IS, TS, and FS for infinite polymeric HCOOH structures can be found in Fig. 6 and the calculated activation

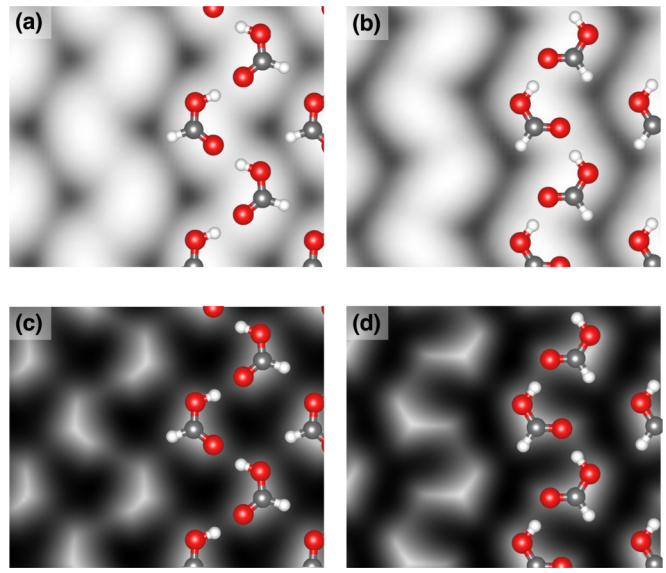

FIG. 5. Simulated STM image of (a) infinite α- and (b) infinite β-polymeric HCOOH images, and simulated AFM image of (c) infinite α- and (d) infinite β-polymeric HCOOH on Cu(111). The bias voltage of +0.2 V was used to simulate the STM images. For the AFM simulations, the CO-functionalized tip was used with the bending stiffness of 0.25 N/m and the effective charge of 0.05 e.

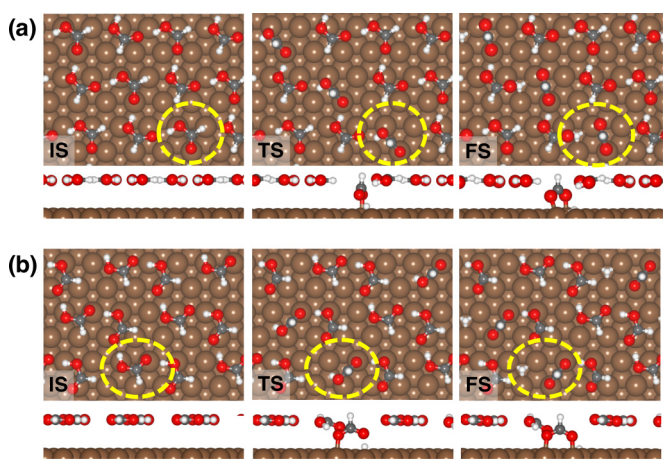

FIG. 6. Molecular configurations for dehydrogenation of (a) infinite α- and (b) infinite β-polymeric HCOOH on Cu(111). IS, TS, and FS indicate initial, transition, and final states, respectively. The yellow dashed circle shows the part of the polymer that is dehydrogenated.

TABLE III. Calculated activation energies for HCOOH dehydrogenation (E_{dec}) in the polymeric structure on Cu(111) along with those for monomeric HCOOH on Cu(111) and experimental value. The zero-point energy correction is not taken into account. The unit of energy is eV.

Structure	Configuration	E_{dec}
Infinite polymer	α	1.25
	β	1.04
Finite polymer	α	0.55
	β	0.45
Monomer	OH-perp	0.62
Expt.		0.67 ± 0.05 [a]

[a]Reference [12].

barriers are summarized in Table III. The calculated activation energies for dehydrogenation (E_{dec}'s) are 1.25 and 1.04 eV for the infinite α- and β-polymeric HCOOHs on Cu(111), respectively, which are larger than that for the monomeric HCOOH dehydrogenation of 0.52 eV. This means that dehydrogenation of the infinite polymeric HCOOH on Cu(111) is kinetically less favorable, because of the hydrogen bonding formed between HCOOH molecules.

We also investigated the dehydrogenation of HCOOH in the finite polymeric HCOOH clusters. Figure 7 shows the minimum energy paths for the finite HCOOH clusters on Cu(111) and the activation energies are summarized in Table III. We examined dehydrogenation from different parts of the cluster and found that the dehydrogenation from the edges that have dangling OH bond are more favorable than those forming hydrogen bonding (see Supplemental Material [41]). The calculated E_{dec}'s for α- and β-polymeric HCOOH's are 0.55 and 0.45 eV, respectively, which are smaller than that for monomeric or infinite polymeric chains, suggesting that

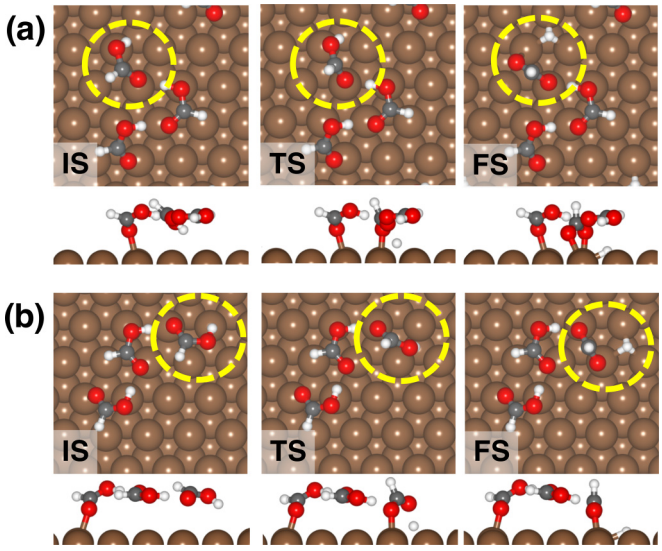

FIG. 7. Molecular configurations for dehydrogenation of (a) finite α- and (b) finite β-polymeric HCOOH clusters on Cu(111). The IS, TS, and FS represent initial state, transition state, and final state, respectively. The yellow dashed circle shows the part of the polymer that is dehydrogenated.

dehydrogenation of HCOOH having an OH bond is favorable and it starts from the edge of the polymeric HCOOH. Our results are consistent with the experimental observation, in which HCOOH decomposition starts from the edges of the polymeric chain, rather than the middle of the chain [10,11].

IV. CONCLUSION

We investigate the adsorption state, electronic and vibrational properties, and catalytic dehydrogenation of polymeric HCOOH structures on Cu(111) surfaces by employing van der Waals inclusive DFT. We present models for the polymeric HCOOHs in the α and β forms on Cu(111), which are approximated by commensurate two-dimensional periodic arrays of the HCOOH molecule with respect to the underlying substrate. We also present finite HCOOH clusters to investigate the effect of the edge in the polymeric HCOOHs on the surface. We found that infinite polymeric HCOOH structures are stabilized by the intermolecular hydrogen bonding and that they interact weakly with the surface. On the other hand, in the finite polymeric clusters, the dangling OH of HCOOH at the edge interacts more strongly with the surface and disrupts the intermolecular interaction. In both infinite and finite polymeric structures, the intermolecular interaction is stronger in the β polymer than in the α polymer, and thus the former is more stable than the latter by about 0.10 eV/HCOOH. We calculated the vibrational frequencies and performed IRAS simulation. The characteristic vibrational frequencies of the out-of-plane π(O−H) and π(C−H) modes for the β-polymeric structure seem to agree with the experiment at first sight, but the relative frequencies and intensities are not consistent with the experiment. On the other hand, the relative vibrational frequencies and peak intensities in the simulated IRAS for the α polymer are consistent and agree better with the experiments [10,12]. Furthermore, our simulated STM and AFM images of the α polymer agree well with the experimental ones by Marcinkowski *et al.* [11] and Shiotari *et al.* [27].

Taken together, although the energetics suggest it is thermodynamically less favorable, we conclude that the α-polymeric HCOOH is likely to be formed on Cu(111). We note that differences of adsorption energies between α and β polymers are small (∼0.1 eV) in both infinite and finite cases, and they are competing energetically. Although rev-vdW-DF2 used in the present work gives the binding energy of the HCOOH dimer comparable to that obtained with the highly accurate coupled cluster method, our results call for the use and/or development of a more accurate electronic structure method to explain the experimental finding more precisely. At present, it is challenging because of the large system size, but we envisage further development of the accurate method capable of simulating a complex interface of the current size.

From the dehydrogenation of HCOOH in the infinite polymeric structures, we found that similar to the monomeric HCOOH, dehydrogenation starts from the OH bond, but the activation barrier is much higher than that of the monomeric one, because of the hydrogen bonding formed between the OH bond and one of the terminal O atoms of the neighboring molecule. On the other hand, the calculated activation energies of the HCOOH having a dangling OH bond in the finite polymeric clusters are smaller, suggesting that the dehydro-

genation starts at the edge of the polymeric structure, not from the middle of it.

In summary, we have clarified the structure of polymeric HCOOH on Cu(111) relevant to the catalytic reaction in the working condition, vibrational property of the polymeric HCOOH, and the active site for the dehydrogenation of HCOOH on Cu(111). We believe our work improves the understanding of the catalytic dehydrogenation of HCOOH and helps develop catalysts used in energy and materials conversion, such as hydrogen production and storage, and methanol synthesis.

ACKNOWLEDGMENTS

S.E.M.P. is supported by the Asahi Glass Foundation Scholarship (AGFS) program during the doctoral course and Indonesia Endowment Fund for Education (LPDP) Scholarship from Ministry of Finance of Indonesia during the master course at Osaka University. The present work was supported by Grants in Aid for Scientific Research on Innovative Areas "Hydrogenomics" (Grants No. JP18H05517 and No. JP18H05519), Scientific Research (B) (Grants No. JP20H02569 and No. JP18H01807), and Transformative Research Areas "Hyperordered Science" (Grant No. JP20H05883) from the Japan Society for the Promotion of Science, the Elements Strategy Initiative for Catalysts and Batteries, supported by the Ministry of Education, Culture, Sports, Science, and Technology, Japan, and GBU-45 Publication Grant, Indonesia. Numerical calculations were partly performed using Super Computers in Institute for Solid State Physics (ISSP), the University of Tokyo.

[1] F. Joó, Breakthroughs in hydrogen storage-formic acid as a sustainable storage material for hydrogen, ChemSusChem **1**, 805 (2008).

[2] L. Yang, X. Hua, J. Su, W. Luo, S. Chen, and G. Cheng, Highly efficient hydrogen generation from formic acid-sodium formate over monodisperse AgPd nanoparticles at room temperature, App. Catal. B **168**, 423 (2015).

[3] A. K. Singh, S. Singh, and A. Kumar, Hydrogen energy future with formic acid: a renewable chemical hydrogen storage system, Catal. Sci. Technol. **6**, 12 (2016).

[4] N. Hoshi, K. Kida, M. Nakamura, M. Nakada, and K. Osada, Structural effects of electrochemical oxidation of formic acid on single crystal electrodes of palladium, J. Phys. Chem. B **110**, 12480 (2006).

[5] J. Scaranto and M. Mavrikakis, Density functional theory studies of HCOOH decomposition on Pd(111), Surf. Sci. **650**, 111 (2016).

[6] N. R. Avery, Adsorption of formic acid on clean and oxygen covered Pt (111), Appl. Surf. Sci. **11**, 774 (1982).

[7] P. Thiel, The reaction of formic acid with clean and water-covered Pt (111), Surf. Sci. **235**, 53 (1990).

[8] J. Scaranto and M. Mavrikakis, HCOOH decomposition on Pt(111): A DFT study, Surf. Sci. **648**, 201 (2016).

[9] W. Sim, P. Gardner, and D. King, Multiple bonding configurations of adsorbed formate on Ag {111}, J. Phys. Chem. **100**, 12509 (1996).

[10] A. E. Baber, K. Mudiyanselage, S. D. Senanayake, A. Beatriz-Vidal, K. A. Luck, E. C. H. Sykes, P. Liu, J. A. Rodriguez, and D. J. Stacchiola, Assisted deprotonation of formic acid on Cu(111) and self-assembly of 1D chains, Phys. Chem. Chem. Phys. **15**, 12291 (2013).

[11] M. D. Marcinkowski, C. J. Murphy, M. L. Liriano, N. A. Wasio, F. R. Lucci, and E. C. H. Sykes, Microscopic view of the active sites for selective dehydrogenation of formic acid on Cu(111), ACS Catal. **5**, 7371 (2015).

[12] Y. Shiozawa, T. Koitaya, K. Mukai, S. Yoshimoto, and J. Yoshinobu, Quantitative analysis of desorption and decomposition kinetics of formic acid on Cu(111): The importance of hydrogen bonding between adsorbed species, J. Chem. Phys. **143**, 234707 (2015).

[13] S. Li, J. Scaranto, and M. Mavrikakis, On the structure sensitivity of formic acid decomposition on cu catalysts, Top. Catal. **59**, 1580 (2016).

[14] M. Columbia, A. Crabtree, and P. Thiel, The temperature and coverage dependences of adsorbed formic acid and its conversion to formate on platinum (111), J. Am. Chem. Soc. **114**, 1231 (1992).

[15] F. Holtzberg, B. Post, and I. Fankuchen, The crystal structure of formic acid, Acta Cryst. **6**, 127 (1953).

[16] I. Nahringbauer, A reinvestigation of the structure of formic acid (at 98 K), Acta Cryst. **34**, 315 (1978).

[17] Y. Mikawa, R. Jakobsen, and J. Brasch, Infrared evidence of polymorphism in formic acid crystals, J. Chem. Phys. **45**, 4750 (1966).

[18] Y. Mikawa, J. Brasch, and R. Jakobsen, Infrared spectra and normal coordinate calculation of crystalline formic acid, J. Mol. Spectrosc. **24**, 314 (1967).

[19] L. C. Grabow and M. Mavrikakis, Mechanism of methanol synthesis on Cu through CO_2 and CO hydrogenation, ACS Catal. **1**, 365 (2011).

[20] S. Singh, S. Li, R. Carrasquillo-Flores, A. C. Alba-Rubio, J. A. Dumesic, and M. Mavrikakis, Formic acid decomposition on Au catalysts: DFT, microkinetic modeling, and reaction kinetics experiments, AIChE J. **60**, 1303 (2014).

[21] J. A. Herron, J. Scaranto, P. Ferrin, S. Li, and M. Mavrikakis, Trends in formic acid decomposition on model transition metal surfaces: A density functional theory study, ACS Catal. **4**, 4434 (2014).

[22] P. Wang, S. N. Steinmann, G. Fu, C. Michel, and P. Sautet, Key role of anionic doping for H_2 production from formic acid on Pd(111), ACS Catal. **7**, 1955 (2017).

[23] J. J. Sims, C. A. Ould Hamou, R. Réocreux, C. Michel, and J. B. Giorgi, Adsorption and decomposition of formic acid on cobalt (0001), J. Phys. Chem. C **122**, 20279 (2018).

[24] S. E. M. Putra, F. Muttaqien, Y. Hamamoto, K. Inagaki, I. Hamada, and Y. Morikawa, Van der Waals density functional study of formic acid adsorption and decomposition on Cu(111), J. Chem. Phys. **150**, 154707 (2019).

[25] B. W. J. Chen and M. Mavrikakis, Formic acid: A hydrogen-bonding cocatalyst for formate decomposition, ACS Catal. **10**, 10812 (2020).

[26] B. W. Chen, S. Bhandari, and M. Mavrikakis, Role of hydrogen-bonded bimolecular formic acid-formate complexes for formic acid decomposition on copper: A combined first-principles and microkinetic modeling study, ACS Catal. **11**, 4349 (2021).

[27] A. Shiotari, S. E. M. Putra, Y. Shiozawa, Y. Hamamoto, K. Inagaki, Y. Morikawa, Y. Sugimoto, J. Yoshinobu, and I. Hamada, Role of intermolecular interactions in the catalytic reaction of formic acid on Cu(111), Small **17**, 2008010 (2021).

[28] https://state-doc.readthedocs.io/.

[29] Y. Morikawa, K. Iwata, J. Nakamura, T. Fujitani, and K. Terakura, Ab initio study of surface structural changes during methanol synthesis over Zn/Cu(111), Chem. Phys. Lett. **304**, 91 (1999).

[30] Y. Morikawa, K. Iwata, and K. Terakura, Theoretical study of hydrogenation process of formate on clean and Zn deposited Cu(111) surfaces, App. Surf. Sci. **169**, 11 (2001).

[31] F. Muttaqien, H. Oshima, Y. Hamamoto, K. Inagaki, I. Hamada, and Y. Morikawa, Desorption dynamics of CO_2 from formate decomposition on Cu(111), Chem. Commun. **53**, 9222 (2017).

[32] D. Vanderbilt, Soft self-consistent pseudopotentials in a generalized eigenvalue formalism, Phys. Rev. B **41**, 7892 (1990).

[33] I. Hamada, van der Waals density functional made accurate, Phys. Rev. B **89**, 121103(R) (2014).

[34] M. Callsen and I. Hamada, Assessing the accuracy of the van der Waals density functionals for rare-gas and small molecular systems, Phys. Rev. B **91**, 195103 (2015).

[35] Y. Hamamoto, I. Hamada, K. Inagaki, and Y. Morikawa, Self-consistent van der Waals density functional study of benzene adsorption on Si(100), Phys. Rev. B **93**, 245440 (2016).

[36] M. Otani and O. Sugino, First-principles calculations of charged surfaces and interfaces: A plane-wave nonrepeated slab approach, Phys. Rev. B **73**, 115407 (2006).

[37] I. Hamada, M. Otani, O. Sugino, and Y. Morikawa, Green's function method for elimination of the spurious multipole interaction in the surface/interface slab model, Phys. Rev. B **80**, 165411 (2009).

[38] Y. Morikawa, Adsorption geometries and vibrational modes of C_2 H_2 on the Si(001) surface, Phys. Rev. B **63**, 033405 (2001).

[39] H. Jónsson, G. Mills, and K. W. Jacobsen, Nudged elastic band method for finding minimum energy paths of transitions, in *Classical and Quantum Dynamics in Condensed Phase Simulations*, edited by B. J. Berne, G. Ciccotti, and D. F. Coker (World Scientific, Singapore, 1998), pp. 385–404.

[40] G. Henkelman, B. P. Uberuaga, and H. Jónsson, A climbing image nudged elastic band method for finding saddle points and minimum energy paths, J. Chem. Phys. **113**, 9901 (2000).

[41] See Supplemental Material at http://link.aps.org/supplemental/10.1103/PhysRevMaterials.5.075801 for further discussion and details of additional results.

[42] S. Hirata, Fast electron-correlation methods for molecular crystals: An application to the α, β_1, and β_2 modifications of solid formic acid, J. Chem. Phys. **129**, 204104 (2008).

[43] J. M. H. Ramón and M. A. Ríos, A new intermolecular polarizable potential for cis-formic acid. Introduction of many-body interactions in condensed phases, Chem. Phys. **250**, 155 (1999).

[44] J. G. Brandenburg, A. Zen, D. Alfé, and A. Michaelides, Interaction between water and carbon nanostructures: How good are current density functional approximations? J. Chem. Phys. **151**, 164702 (2019).

[45] J. Tersoff and D. R. Hamann, Theory and Application for the Scanning Tunneling Microscope, Phys. Rev. Lett. **50**, 1998 (1983).

[46] S. Heinze, S. Blügel, R. Pascal, M. Bode, and R. Wiesendanger, Prediction of bias-voltage-dependent corrugation reversal for STM images of bcc(110) surfaces: W(110), Ta(110), and Fe(110), Phys. Rev. B **58**, 16432 (1998).

[47] M. Rohlfing, R. Temirov, and F. S. Tautz, Adsorption structure and scanning tunneling data of a prototype organic-inorganic interface: PTCDA on Ag (111), Phys. Rev. B **76**, 115421 (2007).

[48] I. Hamada, R. Shimizu, T. Ohsawa, K. Iwaya, T. Hashizume, M. Tsukada, K. Akagi, and T. Hitosugi, Imaging the evolution of *d* states at a strontium titanate surface, J. Am. Chem. Soc. **136**, 17201 (2014).

[49] P. Hapala, G. Kichin, C. Wagner, F. S. Tautz, R. Temirov, and P. Jelínek, Mechanism of high-resolution STM/AFM imaging with functionalized tips, Phys. Rev. B **90**, 085421 (2014).

[50] P. Hapala, R. Temirov, F. S. Tautz, and P. Jelínek, Origin of High-Resolution IETS-STM Images of Organic Molecules with Functionalized Tips, Phys. Rev. Lett. **113**, 226101 (2014).